Editors' Suggestion

Absolutely Stable Spatiotemporal Order in Noisy Quantum Systems

Max McGinley,[1] Sthitadhi Roy,[1,2,3] and S. A. Parameswaran[1]
[1]Rudolf Peierls Centre for Theoretical Physics, Clarendon Laboratory, Oxford University, Parks Road, Oxford OX1 3PU, United Kingdom
[2]Physical and Theoretical Chemistry, Oxford University, South Parks Road, Oxford OX1 3QZ, United Kingdom
[3]International Centre for Theoretical Sciences, Tata Institute of Fundamental Research, Bengaluru 560089, India

(Received 12 January 2022; accepted 28 June 2022; published 24 August 2022)

We introduce a model of nonunitary quantum dynamics that exhibits infinitely long-lived discrete spatiotemporal order robust against any unitary or dissipative perturbation. Ergodicity is evaded by combining a sequence of projective measurements with a local feedback rule that is inspired by Toom's "north-east-center" classical cellular automaton. The measurements in question only partially collapse the wave function of the system, allowing some quantum coherence to persist. We demonstrate our claims using numerical simulations of a Clifford circuit in two spatial dimensions which allows access to large system sizes, and also present results for more generic dynamics on modest system sizes. We also devise explicit experimental protocols realizing this dynamics using one- and two-qubit gates that are available on present-day quantum computing platforms.

DOI: 10.1103/PhysRevLett.129.090404

Introduction.—Quantum systems driven out of equilibrium can exhibit phenomena that have no equilibrium analogues. This has driven a recent thrust aimed at identifying intrinsically nonequilibrium phases of matter in isolated periodically driven quantum many-body systems, which include discrete time crystals (DTCs) [1–5] and Floquet topological phases [6–10]. Each of these phases is characterized by a particular pattern of spatiotemporal order that is infinitely long-lived in the thermodynamic limit, thus necessitating a mechanism for avoiding ergodicity. In locally interacting systems with unitary dynamics, this can be achieved by using spatial disorder to encourage many-body localization (MBL) [11].

The high degree of control offered by quantum simulators makes them a promising platform for experimentally realizing such phases, and progress is already being made in this direction [12,13]. However, with current technology, these platforms inevitably suffer from noise, which destabilizes MBL [14,15]. Therefore, in sufficiently large systems the lifetime of temporal ordering will be noise limited. This presents a question: Given a locally interacting noisy quantum system, what kinds of temporal order can be realised that are (1) infinitely long-lived in the thermodynamic limit, and (2) robust against weak unitary and dissipative perturbations?

Here, we devise a scheme to realize a DTC, using strictly local interactions, that satisfies the above two criteria. Instead of MBL, projective measurements are combined with conditional feedback to evade ergodicity. The measurements we propose do not fully collapse the wave function of the system, thus admitting genuinely quantum dynamics. We show that the resulting spatiotemporal DTC order is absolutely stable against all perturbations [2], including those that break symmetries, and that their correlation time scales exponentially with system size. We devise a protocol to implement this scheme on present-day superconducting quantum processors.

Many-body dynamics in the presence of projective measurements have been extensively explored, particularly with regard to entanglement transitions [16–21]. This generates ensembles of measurement outcomes w and corresponding states ρ_w that can exhibit various orders [22–24]; however, to probe this ensemble experimentally is exponentially hard. Rather than considering the measurement-conditioned states, we use the outcomes of measurements to influence the dynamics itself, in a way that counteracts the deleterious effects of noise.

The DTC we consider here should be distinguished from proposals that use long-range interactions [25–28], fine-tuned dynamical symmetries [29,30], or macroscopically occupied bosonic modes [31,32] to suppress fluctuations, as well as those in zero-dimensional systems [27,33]. Indeed, the spatial dimension of the system, which determines connectivity, plays a key role here. We argue that a measurement-feedback-stabilized DTC is only implementable using local interactions in spatial dimension $d \geq 2$ (without requiring a prohibitively large local state space). This can be compared to an analogous observation for systems subject to time-dependent Lindblad dynamics [34], as well as classical systems [35,36]; we discuss connections between these various protocols.

Measurement-feedback stabilized time crystal.—We consider a system of N qubits on a regular d-dimensional lattice whose dynamics respects discrete time-translation

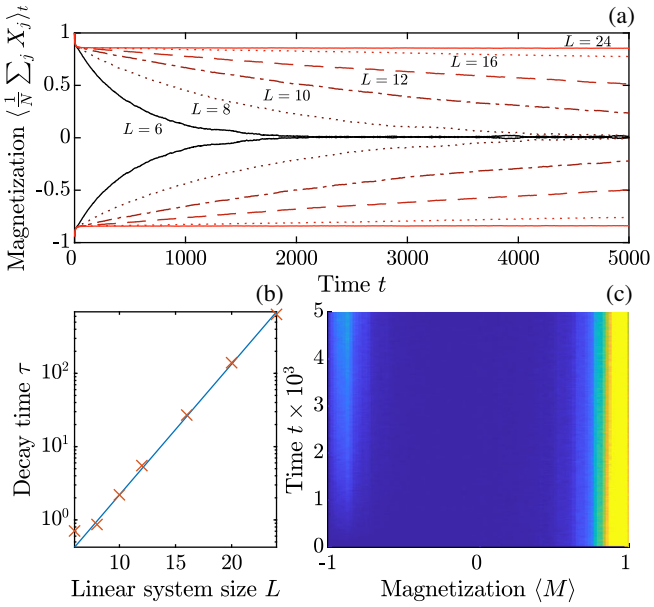

FIG. 1. Oscillations of the magnetization, averaged over 10^4 trajectories, under noisy Clifford dynamics initialized with $\rho(0) = \bigotimes_j |+\rangle\langle+|_j$. (a) Dynamics of magnetization for varying L; even and odd times plotted separately. (b) Estimated decay times τ, extracted by fitting even-time data from (a) to an exponential, plotted against L (red crosses). We find $\tau \propto e^{L/\xi}$ (blue line). (c) Histogram of the even-time sample magnetization for $L = 12$. We fixed $(p_{\text{flip}}, p_{\text{NEC}}, p_{\text{unit}}, p_{\text{reset}}, p_{\text{ME}}) = (0.95, 0.8, 0.02, 0.02, 0.01)$.

symmetry, i.e., the evolution repeats itself after a given time period. The evolution of the density matrix over one such period (which we set to unity) is captured by a quantum channel $\mathcal{N}$ (a completely positive trace-preserving map) such that $\rho(t+1) = \mathcal{N}[\rho(t)]$ (we fix the period to unity). $\mathcal{N}$ plays an analogous role to the Floquet unitary in isolated systems. We split the evolution into two steps: $\mathcal{N} = \mathcal{N}_2 \circ \mathcal{N}_1$. In the first, the qubits are subjected to single-qubit rotations

$$\mathcal{N}_1[\rho] = U_1 \rho U_1^\dagger \qquad U_1 = \prod_j e^{-i\theta_j Z_j/2} \tag{1}$$

where Z_j is the third Pauli matrix acting on qubit j. The variation of θ_j between qubits allows us to describe unintended deviations from some desired pulse angle $\bar{\theta}$, which we presume to be small $|\theta_j - \bar{\theta}| \ll 1$. Later, we will also include incoherent errors during this step.

If $\theta_j = \pi$ for all j then any qubit in the state $|\pm\rangle := (|0\rangle \pm |1\rangle)/\sqrt{2}$ will evolve to $|\mp\rangle$ under (1), giving rise to oscillations of the magnetization $\langle M \rangle := N^{-1}\langle \sum_j X_j \rangle$ with period two. However, deviations of θ_j from π will clearly destroy this subharmonic response in the long time limit. One way to stabilize these otherwise fine-tuned oscillations is to include a second unitary step $\mathcal{N}_2[\rho] = U_2 \rho U_2^\dagger$ where U_2 features strong spatial disorder, driving the system into a Floquet-MBL phase [1,3]. Such a MBL DTC is robust against weak perturbations, provided that the dynamics remains unitary and exactly time periodic [2]. In our case, the stabilization step $\mathcal{N}_2$ is intrinsically nonunitary, and this leads to a DTC of a fundamentally different character. To illustrate how this can be achieved, we first discuss a $d = 1$ setup that fails to fully stabilize a DTC, and then provide a $d = 2$ protocol that succeeds and, *inter alia*, explain the dimensional distinction.

In $d = 1$, a seemingly useful strategy is to perform projective measurements of domain wall operators $W_j := X_j X_{j+1}$. Domain wall measurements provide us with information about the defects incurred by imperfections in $\mathcal{N}_1$, and based on this information we aim to apply operations that systematically remove errors. As mentioned above, we will insist that this feedback be *local*, i.e., we decide what operation to apply to qubit j based only on measurements within some fixed finite distance r from j. Unfortunately, all simple [37] local strategies of this kind fail to simultaneously stabilize two independent steady states in $d = 1$, leading to loss of temporal correlations. The reason is that domain walls can only be eliminated in pairs, making isolated domain walls uncorrectable. Without fine-tuning, there is a nonzero probability that nearby domain walls will separate by a distance $> r$ before they are detected, whereupon they cannot be removed by a local rule. A similar observation has been made for Lindblad dynamics [34].

Instead, we must turn to $d = 2$, where domain walls are linelike, rather than pointlike. Here we *can* define a local feedback rule that successfully removes errors by encouraging closed loops of domain walls to shrink. The rule is closely related to Toom's "north-east-center" (NEC) rule classical cellular automaton, which has provably robust bistability [40]. In the NEC rule, defined on the square lattice, each classical spin is flipped whenever its north and east neighbors are both opposite to itself. Under this update rule, any small domain wall loop will shrink in a south-westerly direction, favoring uniformly ordered states (all 0 s or all 1 s). Our protocol constitutes a quantum version of the NEC rule: For a given qubit we measure domain wall operators $W_{j,\hat{a}} = X_j X_{j+\hat{a}}$, where $\hat{a}$ is either $\hat{n} = (1,0)$ or $\hat{e} = (0,1)$; if both have outcome -1, we apply a π pulse $e^{-i\pi Z_j/2}$. Formally, this operation, which acts on the three qubits j, $j+\hat{n}$, $j+\hat{e}$ can be described by a quantum channel

$$\mathcal{N}_{T,j}[\rho] = \sum_{w_{\hat{n}}, w_{\hat{e}} = \pm 1} U_{w_{\hat{n}}, w_{\hat{e}}} \Pi_{j,\hat{n}}^{w_{\hat{n}}} \Pi_{j,\hat{e}}^{w_{\hat{e}}} \rho \Pi_{j,\hat{e}}^{w_{\hat{e}}} \Pi_{j,\hat{n}}^{w_{\hat{n}}} U_{w_{\hat{n}}, w_{\hat{e}}}^\dagger \tag{2}$$

where $\Pi_{j,\hat{a}}^{w_{\hat{a}}} = (1 + w_{\hat{a}} W_{j,\hat{a}})/2$ projects onto the eigenspace of $W_{j,\hat{a}}$ with eigenvalue $w_{\hat{a}}$, and $U_{w_{\hat{n}}, w_{\hat{e}}}$ is the conditional unitary, which equals $e^{-i\pi Z_j/2}$ if $w_{\hat{n}} = w_{\hat{e}} = -1$, and $\mathbb{I}$ otherwise. This channel outputs a density matrix that is

a classical mixture of all possible outcomes. In principle, we could examine the full ensemble of states conditioned on measurement outcomes by "unravelling" the channel [19] and examining the ensemble $\{(p_{\vec{w}}, \rho_{\vec{w}})\}$, where $\vec{w}$ is a measurement history, $p_{\vec{w}}$ is its probability, and $\rho_{\vec{w}}$ is the state conditioned on $\vec{w}$. However, sampling the full space of measurement outcomes is exponentially hard, so we instead focus on the mixture (2).

In the full stabilization step $\mathcal{N}_2$, we choose to apply the measurement-feedback sequence $\mathcal{N}_{T,j}$ to each qubit in a particular sublattice $j \in A$ independently with probability p_{NEC}; we then do the same for the opposite sublattice B. (Note that $\{\mathcal{N}_{T,j}\}$ do not necessarily commute on different sublattices.). Formally, we have $\mathcal{N}_2 = \prod_{j\in B}[(1-p_{\mathrm{NEC}}) + p_{\mathrm{NEC}}\mathcal{N}_{T,j}] \prod_{j\in A}[(1-p_{\mathrm{NEC}}) + p_{\mathrm{NEC}}\mathcal{N}_{T,j}]$. The maximum error correction rate occurs at $p_{\mathrm{NEC}} = 1$.

Numerical simulations.—We now test these ideas using numerical simulations in two ways. First, we employ Clifford circuitry, which involves a restricted range of operations that can be simulated efficiently for large system sizes [41]. The allowed unitary and nonunitary operations are sufficiently diverse, allowing us to verify the robust nature of the spatiotemporal order. Second, for modest L we simulate circuits with arbitrary gates; these results are described in the Supplemental Material [43].

The full sequence of operations in the Clifford circuits is as follows. In place of partial rotations $\theta_j \neq \pi$, we apply π pulses to each spin with some probability p_{flip}. Then, for each qubit j, a two-qubit gate $e^{-i\pi Z_j Z_{j'}/4}$ is applied with probability p_{unit} for some randomly chosen neighbor j'. Qubits are then reset into the $|+\rangle_j$ at random with probability p_{reset} (note that this explicitly breaks the Ising $+X_j \leftrightarrow -X_j$ symmetry). Finally, the correction step $\mathcal{N}_2$ is made. We model measurement errors by inverting measurement outcomes with probability p_{ME} before deciding whether or not to apply the correcting π pulse. In all data, averages over the measurement outcomes and random decisions are performed simultaneously.

To probe DTC order, we initialize the system in an $X_j = 1$ eigenstate for all j, and calculate the expectation value of the magnetization $\langle M\rangle_t = \langle (1/N)\sum_j X_j\rangle$ after t time steps. For nonzero but sufficiently small error probabilities $(p_{\mathrm{unit}}, p_{\mathrm{reset}}, p_{\mathrm{ME}})$, we see the hallmark period-doubled oscillations [Fig. 1(a)], with an amplitude that quickly reaches a quasistationary value after some $O(1)$ time. In finite-size systems the oscillations eventually decay at late times, but the timescale of this decay τ grows exponentially with the linear system size L [Fig. 1(b)]. The distribution of magnetization M [Fig. 1(c)] remains bimodal, implying that the decay is due to rare events where the sign of the magnetization flips across the entire system. Such processes require domain walls to traverse the system before being corrected, which requires $O(L)$ spin-flips in an $O(1)$ time, explaining the dependence of τ on L. Thus, despite the presence of noise, these oscillations are infinitely long-lived in the thermodynamic limit. We have confirmed that the same oscillations are seen for generic, partially magnetized initial states [43], and when the two-qubit unitaries are replaced by random Clifford gates, and decoherence in the Z basis is included.

A more rigorous way to identify a time crystal is to look for spatiotemporal order [52], conveniently probed by the correlator $C_t(j,j') \coloneqq \langle X_j(t) X_{j'}(0)\rangle$, where the operator $X_j(t) = (\mathcal{N}^\dagger)^t[X_j]$ evolves in the Heisenberg picture, and the expectation value is taken with respect to a steady state of the dynamics. We have confirmed that $C_t(j,j')$ approaches a nonzero value whose value oscillates with period two as $|j-j'| \to \infty$ [43], indicating that the characteristic DTC order is robust in the thermodynamic limit.

The same quantities can be used to identify other phases in the parameter space. If the pulse angles θ_j are close to 0 rather than π (or the flip rate p_{flip} is small), then the magnetization will not oscillate, instead reaching a static value. When noise is sufficiently weak, this saturation value depends on the initial state, which implies that the time evolution channel $\mathcal{N}$ has multiple steady states in the thermodynamic limit, spanned by two density matrices $\rho_{\mathrm{ss},+}$, $\rho_{\mathrm{ss},-}$ that correspond to opposite signs of magnetization. We refer to this phase as a ferromagnet (although unlike conventional ferromagnets, this behavior is robust against perturbations that break the Ising symmetry, e.g., resets in the Clifford circuits described above). If noise is increased, or the correction rate p_{NEC} is reduced, then eventually this bistability is lost, leading to a paramagnetic phase where the magnetization reaches a static, initial-state-independent value. A qualitative phase diagram is shown in Fig. 2(a).

Transitions between adjacent phases [paramagnetic (PM) to ferromagnetic (FM) or DTC] can be driven by a number of different parameters. An example of particular interest is the entangling unitary gates, occurring with probability p_{unit}. The scrambling nature of these processes encourages internal thermalization, where local subsystems equilibrate by becoming entangled with the rest of the system; thus we expect that chaotic unitary evolution competes with the nonergodic FM and DTC phases. We find that the system remains nonergodic up to a finite value of p_{unit}, where a transition to the PM phase occurs. We find critical behaviour consistent with the Ising universality class [43]. Note that the DTC-PM transition in a noisy, driven, classical spin system is in the same universality class [53], despite the DTC being a genuine nonequilibrium state.

Experimental implementation.—Finally, we demonstrate that our DTC can be experimentally realized using resources that are currently available in most superconducting qubit quantum computers with two-dimensional architectures. Our proposal requires single-qubit rotations and measurements combined with one entangling gate, which we take to

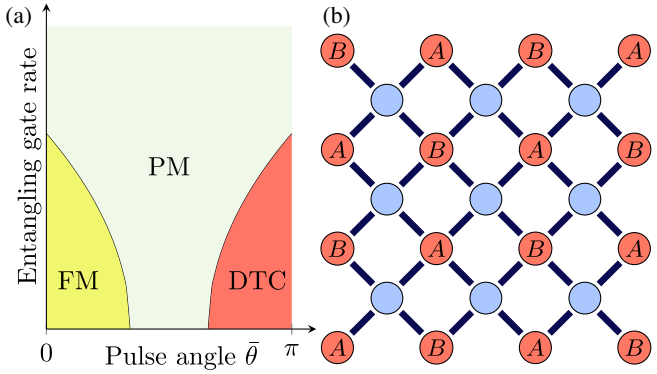

FIG. 2. (a) Qualitative phase diagram as a function of the mean pulse angle $\bar{\theta}$ [Eq. (1)] and the strength of entangling unitary evolution. We distinguish the paramagnetic (PM) phase, where the system equilibrates and the steady state is unique, from the ferromagnetic (FM) and discrete time-crystalline (DTC) phases, which in the thermodynamic limit are nonergodic, with persistent oscillations in the latter case. The DTC exhibits period-doubled oscillations in magnetization and autocorrelators, while these quantities reach a time-independent value in the FM phase. (b) Geometry of a superconducting processor that realizes the measurement-feedback stabilized DTC. System qubits (red circles) that exhibit DTC order are capacitively coupled (solid lines) to ancillas (blue circles), facilitating the necessary measurements.

be CNOT. (Gates equivalent to CNOT up to single-qubit unitaries, including CZ [54,55] and cross-resonance [56,57], also suffice.)

Qubits are arranged on a square lattice with nearest-neighbor connectivity [Fig. 2(b)]. The "system" qubits on one sublattice (dark red) will exhibit DTC order, and are coupled to ancillas on the opposite sublattice (light blue). The system sites form a larger square lattice; evidently, any pair of neighboring system qubits are coupled to least one shared ancilla. To measure $W_{j,\hat{n}}$, we prepare ancilla b that is connected to both j and $j+\hat{n}$ in the state $|+\rangle_b$, and apply $\mathrm{CNOT}_{b\to j}$, followed by $\mathrm{CNOT}_{b\to j+\hat{n}}$ ($\mathrm{CNOT}_{c\to t}$ is a CNOT with c, t as control and target, respectively). Finally, the ancilla is measured in the X_b basis. We may verify [43] that an outcome $X_b = \pm 1$ projects the state onto the subspace $W_{j,\hat{n}} = \mp 1$, as desired. The same procedure can be used to measure $W_{j,\hat{e}}$, and the feedback gate can then be applied if both outcomes are -1, thus simulating the channel (2).

Our simulations so far have featured periodic boundary conditions, however, this is not always possible to implement in experiments. The NEC rule will sometimes fail to correct errors if naïvely generalized to open boundary conditions [58], due to corners without north or east neighbors. The simplest remedy is to switch to a majority vote rule, where all four domain wall operators adjacent to a site j are measured and the π pulse is applied if at least two domain walls are present. The corresponding classical cellular automaton exhibits robust bistability with open boundaries; thus we expect that such a quantum feedback rule will stabilize a DTC. Unlike the NEC rule, the majority vote respects detailed balance, suggesting that the error elimination mechanism will be slower [59], and that true bistability may be compromised in the ferromagnetic phase if the $X_j \to -X_j$ $\mathbb{Z}_2$ symmetry is broken [60]. (In the DTC phase, any up-down bias incurred in one time step is canceled out in the next.) Alternatively, we may retain the advantages of the NEC rule with open boundaries by employing an unusual annular geometry [43].

Projective measurements of superconducting qubits are typically slow compared to gate times. In IBM's current cloud-based quantum devices, the readout time is ~ 5 μs, while the T_1, T_2 times are ~ 100 μs [61]. Thus, the effective error rate per layer will be of order 5%. Using Clifford circuits, we have confirmed that a DTC can be stabilized even with depolarizing errors as high as this, assuming measurement errors of 1% and the same $p_{\mathrm{NEC}} = 0.8$ as in Fig. 1. As an alternative, in the Supplemental Material [43] we suggest a method to implement the same channel (2) using purely quantum gates and qubit resets, the latter of which can be done much faster (250 ns in Ref. [62]).

Discussion.—In closing, it is helpful to compare our model with analogous systems that use engineered Lindblad dynamics as an entropy drain for stabilizing DTCs [34]. Although Lindbladians are defined on continuous rather than discrete time, it is possible to qualitatively compare the two by considering the Lindblad dynamics using quantum jump trajectories [63], built up of Poisson-distributed discrete "jump events". The jump operators in Ref. [34] are chosen according to a majority vote with all four neighbors. One example is $L_{j,\vec{b}} = |b_j b_n b_e b_s b_w\rangle\langle \bar{b}_j b_n b_e b_s b_w|$, where $b \in \{+,-\}$, $\bar{b} := -b$, and n, e, s, w are the north, east, south, and west neighbors of j, respectively. After a jump event $|\psi\rangle \to L_{j,\vec{b}}|\psi\rangle$, the state of the five qubits involved is projected into a product of X_j eigenstates. This differs in a crucial way from the measurement-feedback loop in our model: Domain wall operators are measured rather than individual qubit X_j operators, which means that some quantum coherence can be preserved. For instance, if the three qubits c, e, n involved in $\mathcal{N}_{T,j}$ [Eq. (2)] begin in the superposition state $\alpha|-_c+_e+_n\rangle + \beta|+_c-_e-_n\rangle$, then the output state will be $\alpha|+_c+_e+_n\rangle + \beta|-_c-_e-_n\rangle$, which is also coherent. As a result, the steady states of the channel $\mathcal{N}_2$ form a coherent subspace: Any state within the Bloch sphere spanned by the pure states $|+^{\otimes N}\rangle$, $|-^{\otimes N}\rangle$ is unaffected by $\mathcal{N}_2$, which implies the existence of a decoherence-free subspace [64]. In contrast, if we measured X_j operators, or used the Lindblad model of Ref. [34], then only incoherent mixtures $(1-p)|+^{\otimes N}\rangle\langle+^{\otimes n}| + p|-^{\otimes N}\rangle\langle-^{\otimes n}|$ would be stabilized. (For a more detailed comparison of the two kinds of dynamics, it is useful to take a continuum time limit of our model [43].) Other practical differences are that the discrete measurement-feedback process needn't be active

during the pulse step $\mathcal{N}_1$; also, in most experimental platforms with single-site control, conditional feedback is easier to achieve than the reservoir engineering required by the Lindblad approach.

In practice, the massively multipartite entanglement contained in macroscopic coherent superpositions ("cat states") will be susceptible to noisy perturbations. Thus, we expect that classical information (the sign of the initial magnetization) will preserved for arbitrarily long $[T_1 \to \infty]$ times, while quantum information will persist over a noise-limited $[T_2]$ timescale. In the language of quantum error correction, $\mathcal{N}_2$ constitutes a strictly local implementation of a repetition code [65], and so either X-type or Z-type errors can be corrected, not both. Other classical cellular automata have also been used as a basis for local implementations of different quantum codes [66].

Very recent work has leveraged the NEC rule to realize absolutely stable time-crystalline order in classical Hamiltonian systems with Langevin noise [36]. Our results show that reliable classical automata such as the NEC rule are also stable against quantum fluctuations, generated by, e.g., entangling unitary gates, up to some finite rate [see Fig. 2(a)]. The bistability of the classical automaton in question translates to the existence of robust multiple steady states of the quantum channel $\mathcal{N}_2$. Each steady state forms a basin of attraction for the dynamics [28], and the pulses in $\mathcal{N}_1$ map states in the basin of one attractor to that of the other.

Our study highlights the potential of measurement-feedback loops for synthesizing interesting kinds of non-unitary dynamics, which can be probed experimentally without issues of scalability. This strategy can be seen as a useful alternative to reservoir engineering [67] that is particularly appropriate for systems with single-qubit control. We look forward to investigating the interplay between this paradigm of dynamics and other kinds of quantum nonequilibrium phases of matter.

In compliance with EPSRC policy framework on research data, this publication is theoretical work that does not require supporting research data.

We thank A. Daley for discussions, and M. Ippoliti for helpful comments on the manuscript. We acknowledge support from UK Engineering and Physical Sciences Research Council Grant No. EP/S020527/1. S. R. also acknowledges support from an ICTS-Simons Early Career Faculty Fellowship via a grant from the Simons Foundation (677895, R. G.)

[1] V. Khemani, A. Lazarides, R. Moessner, and S. L. Sondhi, Phase Structure of Driven Quantum Systems, Phys. Rev. Lett. **116**, 250401 (2016).

[2] C. W. von Keyserlingk, V. Khemani, and S. L. Sondhi, Absolute stability and spatiotemporal long-range order in floquet systems, Phys. Rev. B **94**, 085112 (2016).

[3] D. V. Else, B. Bauer, and C. Nayak, Floquet Time Crystals, Phys. Rev. Lett. **117**, 090402 (2016).

[4] R. Moessner and S. L. Sondhi, Equilibration and order in quantum floquet matter, Nat. Phys. **13**, 424 (2017).

[5] N. Y. Yao, A. C. Potter, I.-D. Potirniche, and A. Vishwanath, Discrete Time Crystals: Rigidity, Criticality, and Realizations, Phys. Rev. Lett. **118**, 030401 (2017).

[6] M. S. Rudner, N. H. Lindner, E. Berg, and M. Levin, Anomalous Edge States and the Bulk-Edge Correspondence for Periodically Driven Two-Dimensional Systems, Phys. Rev. X **3**, 031005 (2013).

[7] A. C. Potter, T. Morimoto, and A. Vishwanath, Classification of Interacting Topological Floquet Phases in One Dimension, Phys. Rev. X **6**, 041001 (2016).

[8] D. V. Else and C. Nayak, Classification of topological phases in periodically driven interacting systems, Phys. Rev. B **93**, 201103(R) (2016).

[9] C. W. von Keyserlingk and S. L. Sondhi, Phase structure of one-dimensional interacting floquet systems. I. Abelian symmetry-protected topological phases, Phys. Rev. B **93**, 245145 (2016).

[10] R. Roy and F. Harper, Periodic table for floquet topological insulators, Phys. Rev. B **96**, 155118 (2017).

[11] R. Nandkishore and D. A. Huse, Many-body localization and thermalization in quantum statistical mechanics, Annu. Rev. Condens. Matter Phys. **6**, 15 (2015).

[12] M. Ippoliti, K. Kechedzhi, R. Moessner, S. L. Sondhi, and V. Khemani, Many-body physics in the nisq era: Quantum programming a discrete time crystal, PRX Quantum **2**, 030346 (2021).

[13] X. Mi *et al.*, Time-crystalline eigenstate order on a quantum processor, Nature (London) **601**, 531 (2022).

[14] R. Nandkishore, S. Gopalakrishnan, and D. A. Huse, Spectral features of a many-body-localized system weakly coupled to a bath, Phys. Rev. B **90**, 064203 (2014).

[15] S. Johri, R. Nandkishore, and R. N. Bhatt, Many-Body Localization in Imperfectly Isolated Quantum Systems, Phys. Rev. Lett. **114**, 117401 (2015).

[16] Y. Li, X. Chen, and M. P. A. Fisher, Quantum zeno effect and the many-body entanglement transition, Phys. Rev. B **98**, 205136 (2018).

[17] Y. Li, X. Chen, and M. P. A. Fisher, Measurement-driven entanglement transition in hybrid quantum circuits, Phys. Rev. B **100**, 134306 (2019).

[18] Y. Bao, S. Choi, and E. Altman, Theory of the phase transition in random unitary circuits with measurements, Phys. Rev. B **101**, 104301 (2020).

[19] M. J. Gullans and D. A. Huse, Dynamical Purification Phase Transition Induced by Quantum Measurements, Phys. Rev. X **10**, 041020 (2020).

[20] R. Fan, S. Vijay, A. Vishwanath, and Y.-Z. You, Self-organized error correction in random unitary circuits with measurement, Phys. Rev. B **103**, 174309 (2021).

[21] M. Ippoliti, M. J. Gullans, S. Gopalakrishnan, D. A. Huse, and V. Khemani, Entanglement Phase Transitions in Measurement-Only Dynamics, Phys. Rev. X **11**, 011030 (2021).

[22] A. Lavasani, Y. Alavirad, and M. Barkeshli, Measurement-induced topological entanglement transitions in symmetric random quantum circuits, Nat. Phys. **17**, 342 (2021).

[23] S. Sang and T. H. Hsieh, Measurement-protected quantum phases, Phys. Rev. Research **3**, 023200 (2021).
[24] Y. Bao, S. Choi, and E. Altman, Symmetry enriched phases of quantum circuits, Ann. Phys. **435**, 168618 (2021).
[25] A. Russomanno, F. Iemini, M. Dalmonte, and R. Fazio, Floquet time crystal in the lipkin-meshkov-glick model, Phys. Rev. B **95**, 214307 (2017).
[26] S. Choi, J. Choi, R. Landig, G. Kucsko, H. Zhou, J. Isoya, F. Jelezko, S. Onoda, H. Sumiya, V. Khemani *et al.*, Observation of discrete time-crystalline order in a disordered dipolar many-body system, Nature (London) **543**, 221 (2017).
[27] Z. Gong, R. Hamazaki, and M. Ueda, Discrete Time-Crystalline Order in Cavity and Circuit QED Systems, Phys. Rev. Lett. **120**, 040404 (2018).
[28] F. M. Gambetta, F. Carollo, M. Marcuzzi, J. P. Garrahan, and I. Lesanovsky, Discrete Time Crystals in the Absence of Manifest Symmetries or Disorder in Open Quantum Systems, Phys. Rev. Lett. **122**, 015701 (2019).
[29] B. Buča, J. Tindall, and D. Jaksch, Non-stationary coherent quantum many-body dynamics through dissipation, Nat. Commun. **10**, 1730 (2019).
[30] K. Chinzei and T. N. Ikeda, Time Crystals Protected by Floquet Dynamical Symmetry in Hubbard Models, Phys. Rev. Lett. **125**, 060601 (2020).
[31] J. Smits, L. Liao, H. T. C. Stoof, and P. van der Straten, Observation of a Space-Time Crystal in a Superfluid Quantum Gas, Phys. Rev. Lett. **121**, 185301 (2018).
[32] A. Pizzi, J. Knolle, and A. Nunnenkamp, Period-n Discrete Time Crystals and Quasicrystals with Ultracold Bosons, Phys. Rev. Lett. **123**, 150601 (2019).
[33] K. Sacha, Modeling spontaneous breaking of time-translation symmetry, Phys. Rev. A **91**, 033617 (2015).
[34] A. Lazarides, S. Roy, F. Piazza, and R. Moessner, Time crystallinity in dissipative floquet systems, Phys. Rev. Research **2**, 022002(R) (2020).
[35] N. Y. Yao, C. Nayak, L. Balents, and M. P. Zaletel, Classical discrete time crystals, Nat. Phys. **16**, 438 (2020).
[36] Q. Zhuang, F. Machado, N. Y. Yao, and M. P. Zaletel, An absolutely stable open time crystal, arXiv:2110.00585.
[37] There may exist a feedback strategy in $d = 1$ that mimics the dynamics of Gaçs' classical automaton [38,39]; however the only known protocols of this kind require a local state space of dimension order 2^{400}, which we rule out as infeasible.
[38] P. Gács, Reliable computation with cellular automata, J. Comput. Syst. Sci. **32**, 15 (1986).
[39] L. F. Gray, A reader's guide to gacs's "positive rates" paper, J. Stat. Phys. **103**, 1 (2001).
[40] A. Toom, Stable and attractive trajectories in multicomponent systems, in *Multicomponent Random Systems* (Marcel Dekker, New York, 1980), pp. 549–575.
[41] Simulations were performed using the STIM package [42], version 1.4.0.
[42] C. Gidney, Stim: A fast stabilizer circuit simulator, Quantum **5**, 497 (2021).
[43] See Supplemental Material at http://link.aps.org/supplemental/10.1103/PhysRevLett.129.090404 for a detailed comparison with the continuum-time dynamics of Ref. [34]; a construction of the quantum NEC rule with open boundaries; an analysis of the experimental domain wall measurement procedure; and details of non-Clifford dynamics simulations, which includes Refs. [44–51].
[44] H. Breuer and F. Petruccione, *The Theory of Open Quantum Systems* (Oxford University Press, New York, 2002).
[45] G. Grinstein, Can complex structures be generically stable in a noisy world?, IBM J. Res. Dev. **48**, 5 (2004).
[46] A. Kubica and J. Preskill, Cellular-Automaton Decoders with Provable Thresholds for Topological Codes, Phys. Rev. Lett. **123**, 020501 (2019).
[47] T. Sleator and H. Weinfurter, Realizable Universal Quantum Logic Gates, Phys. Rev. Lett. **74**, 4087 (1995).
[48] K. Binder, Finite size scaling analysis of ising model block distribution functions, Z. Phys. B Condens. Matter **43**, 119 (1981).
[49] U. C. Täuber, V. K. Akkineni, and J. E. Santos, Effects of Violating Detailed Balance on Critical Dynamics, Phys. Rev. Lett. **88**, 045702 (2002).
[50] S. V. Isakov, P. Fendley, A. W. W. Ludwig, S. Trebst, and M. Troyer, Dynamics at and near conformal quantum critical points, Phys. Rev. B **83**, 125114 (2011).
[51] M. P. Nightingale and H. W. J. Blöte, Monte carlo computation of correlation times of independent relaxation modes at criticality, Phys. Rev. B **62**, 1089 (2000).
[52] V. Khemani, C. W. von Keyserlingk, and S. L. Sondhi, Defining time crystals via representation theory, Phys. Rev. B **96**, 115127 (2017).
[53] F. M. Gambetta, F. Carollo, A. Lazarides, I. Lesanovsky, and J. P. Garrahan, Classical stochastic discrete time crystals, Phys. Rev. E **100**, 060105(R) (2019).
[54] B. Foxen *et al.* (Google AI Quantum), Demonstrating a Continuous Set of Two-Qubit Gates for Near-Term Quantum Algorithms, Phys. Rev. Lett. **125**, 120504 (2020).
[55] F. Arute, K. Arya, R. Babbush, D. Bacon, J. C. Bardin, R. Barends, R. Biswas, S. Boixo, F. G. Brandao, D. A. Buell *et al.*, Quantum supremacy using a programmable superconducting processor, Nature (London) **574**, 505 (2019).
[56] J. M. Chow, A. D. Córcoles, J. M. Gambetta, C. Rigetti, B. R. Johnson, J. A. Smolin, J. R. Rozen, G. A. Keefe, M. B. Rothwell, M. B. Ketchen, and M. Steffen, Simple All-Microwave Entangling Gate for Fixed-Frequency Superconducting Qubits, Phys. Rev. Lett. **107**, 080502 (2011).
[57] A. D. Patterson, J. Rahamim, T. Tsunoda, P. A. Spring, S. Jebari, K. Ratter, M. Mergenthaler, G. Tancredi, B. Vlastakis, M. Esposito, and P. J. Leek, Calibration of a Cross-Resonance Two-Qubit Gate between Directly Coupled Transmons, Phys. Rev. Applied **12**, 064013 (2019).
[58] M. Vasmer, D. E. Browne, and A. Kubica, Cellular automaton decoders for topological quantum codes with noisy measurements and beyond, Sci. Rep. **11**, 2027 (2021).
[59] C. H. Bennett and G. Grinstein, Role of Irreversibility in Stabilizing Complex and Nonergodic Behavior in Locally Interacting Discrete Systems, Phys. Rev. Lett. **55**, 657 (1985).
[60] C. H. Bennett, G. Grinstein, Y. He, C. Jayaprakash, and D. Mukamel, Stability of temporally periodic states of classical many-body systems, Phys. Rev. A **41**, 1932 (1990).
[61] IBM quantum services, https://quantum-computing.ibm.com/services?services=systems (accessed 30th Oct. 2021).

[62] M. McEwen, D. Kafri, Z. Chen, J. Atalaya, K. Satzinger, C. Quintana, P. V. Klimov, D. Sank, C. Gidney, A. Fowler *et al.*, Removing leakage-induced correlated errors in superconducting quantum error correction, Nat. Commun. **12**, 1 (2021).

[63] J. Dalibard, Y. Castin, and K. Mølmer, Wave-Function Approach to Dissipative Processes in Quantum Optics, Phys. Rev. Lett. **68**, 580 (1992).

[64] D. A. Lidar, I. L. Chuang, and K. B. Whaley, Decoherence-Free Subspaces for Quantum Computation, Phys. Rev. Lett. **81**, 2594 (1998).

[65] M. A. Nielsen and I. L. Chuang, *Quantum Computation and Quantum Information: 10th Anniversary Edition* (Cambridge University Press, Cambridge, England, 2010).

[66] J. Harrington, Analysis of quantum error-correcting codes: Symplectic lattice codes and toric codes, Ph.D. thesis, California Institute of Technology, 2004, 10.7907/AHMQ-EG82.

[67] J. F. Poyatos, J. I. Cirac, and P. Zoller, Quantum Reservoir Engineering with Laser Cooled Trapped Ions, Phys. Rev. Lett. **77**, 4728 (1996).